Clinical application of EIT system for static imaging of thorax

V Cherepenin[1], A Karpov[2], A Korjenevsky[1], V Kornienko[1], Yu Kultiasov[1], A Mazaletskaya[3] and D Mazourov[4]

[1]Institute of Radio-Engineering and Electronics of Russian Academy of Sciences, Moscow, Russia
[2]Clinical Hospital No 9, Yaroslavl, Russia
[3]Yaroslavl State University, Russia
[4]Regional Oncological Hospital, Yaroslavl, Russia

Classification numbers: 87.63.-d, 87.63.Pn

Keywords: electrical impedance tomography, lung diagnostics, bio-impedance, medical imaging.

[1] E-mail: korjenevsky@cplire.ru
[3] E-mail: almaz@yars.free.net

Abstract. Results of clinical evaluation of one-frequency electrical impedance tomography (EIT) system enabling static *in vivo* imaging are presented. Design of the measuring system and software are described shortly. EIT images of human chest in norm and with various abnormalities are given and discussed. The evaluated system distinguishably visualises various states of lungs and thorax including lung cancer. In spite of low resolution the method demonstrates sensitivity to lung cancer. Suggested explanation of this fact is decreasing of aeration of affected lung due to bronchus narrowing and corresponding decreasing of impedance of large areas inside lung.

Introduction

Electrical impedance tomography (EIT) providing safe non-invasive way to visualise electrical properties of tissues inside human body was introduced by Barber and Brown in the eighties (Barber and Brown 1984). Different tissues of human body have different electrical properties so the imaging of anatomical structures is possible by EIT. Abnormal tissues, in particular tumours, demonstrate electrical impedance distinguishing from surrounding sound tissues and this fact can be applied for medical diagnosis. Both tasks expect possibility of EIT system to image static objects inside human body. Till the recent time the EIT was able to produce only so-called dynamic images, i.e. images of conductivity changes occurred between two consequent measurements. Static imaging with satisfactory quality was limited by the difficulty of inverse problem solving when neither exact geometry of boundary surface of the object, nor the arrangement of measuring electrodes on this surface are known. This limitation hindered implementation of EIT in clinical practice. Development of fast and robust static EIT reconstruction method and efficient measuring equipment (Korjenevsky 1995, Cherepenin *et al* 1995, Korjenevsky *et al* 1997) allows overcoming this problem.

The problem of lung diagnosis by EIT methods was considered in a number of publications (Harris *et al* 1987, Leathard *et al* 1994, Eyuboglu *et al* 1995, Frerichs *et al* 1999 and others). In some cases the dynamic (differential) nature of available images restricted clinical application of EIT technique. For example the tumors are static (very slow) objects invisible directly by means of dynamic EIT. We present here the results of comparative assessment of static EIT images for lungs at norm and with various abnormalities including cancer. In spite of low spatial resolution the method demonstrates sensitivity to lung cancer. Possible explanation of this data is suggested.

Materials and Methods

2.1 Measuring system

Examinations were made with 16-electrodes one-frequency (8 kHz) electrical impedance tomography system, created in Institute of Radio-Engineering and Electronics, Russian Academy of Sciences (Korjenevsky *et al* 1997). The multiplexed single channel architecture of measuring system and polar current injection strategy are used. The amplitude of injected current is approximately 0.5 mA. A full data set consisting of 192 potential differences between adjacent non-injecting electrodes is acquired during 90 ms. The injected current has rectangular pulse waveform. An analogue synchronous detector and switchable integrator convert AC potential differences under measurement to DC before analogue to digital conversion in voltmeter. The feedback involving common mode output of voltmeter's instrumental amplifier and voltage output of current source reduces common mode of the input signal to the negligible value at any combination of injecting and measuring electrodes. Fast-response circuit for galvanic potential compensation enables reliable measurements with stainless steel or aluminium electrodes. The measuring system is mounted in compact 320x250x55 mm all-metal case.

2.2 Reconstruction software

The reconstruction algorithm is based on weighted back projection. The main advantage of developed method is possibility of fast reconstruction of static conductivity without exact knowledge of body shape and arrangement of electrodes. The algorithm is applicable both for adjacent (dipole) current injection (Korjenevsky 1995) and for non-adjacent injection (Korjenevsky *et al* 1998). The idea of method is in the synthesis of reference data set, corresponding to a homogeneous body with the same arrangement of electrodes, from the actually measured data. Such reference data can be utilised then for back projection reconstruction of static conductivity distribution inside object. The reference data are created by the weighted least squares approximation of measured data with the set of smooth linearly independent functions. This enables to keep in approximation general trends of measured data related with the body shape and electrodes distribution rather than fine-scale details bearing information on the object's internal structure. The best results are obtained with the formula:

$$u_r^i(j) = c_1^i f^i(j) + c_2^i,$$

where $u_r^i(j)$ - synthesised reference data set, i - count of current pattern, j - count of measuring pair of electrodes, $f^i(j)$ - distribution of voltage between adjacent electrodes on the surface of simple reference object such as homogeneous conductive cylinder, which can be calculated analytically, $c_{1,2}^i$ - approximation coefficients, calculated by the weighted least squares method.

The quantitative data, which can be obtained from reconstructed conductivity distributions, are not real values of conductivity because of artificial nature of reference data set and limitations of linear back projection reconstruction. To fix at least one point on the scale, the reconstruction software can operate in "scale" mode, when it tries to find spine bone on the picture and then shifts all values on the image in such a way that "conductivity" of the bone gets zero value.

The time required for the reconstruction of a single static conductivity distribution is less than 10 ms with Pentium 233 MHz processor. Taking into account data collection rate this enables 11 frames per second real time imaging using standard PC.

2.3 Clinical measurements

For thorax measurements we used circle aluminium electrodes with 20 mm diameter, fixed on elastic rubber belt. ECG-gel was used for better electrodes' contact with patient's skin. 31 male persons were examined and divided into 4 clinical groups. First group was formed of 22 patients with clinical diagnosis lung's cancer with tumour localisation in one lung. Second group consisted of 7 healthy persons. One patient after one-sided pneumoektomia and one patient with diagnosis one-side emphysema were examined also. Clinical diagnoses were affirmed by pre-surgery x-rays investigations where applicable. The average age of patients was 58 years. Examinations were made in standing position only. EIT scanning of thorax was made in three horizontal planes: 3-rd intercostal space, 4-th intercostal space, 5-th intercostal space. For correct estimation we compared tomographic images got from the same scanning plane. All examinations and all were made in standard conditions: from 9 to 12 a.m. in room with normal air humidity and temperature 20-22°C, in standing position after relaxation. Duration of patient examination (electrodes application, measurements, image processing) was about 10 min. The EIT measurements were performed during spontaneous breathing of patient using "movie" mode with zero delays between frames. In this mode device carries out continuous measurements during specified period (20 sec) with 11 frames/s rate. For the purposes of described research, one of the frames corresponding to maximum aeration of lungs (estimated visually from EIT

images) was chosen for further evaluation. The least value of conductivity inside lung area was taken for statistical comparison of average lung conductivity in different groups.

The analysis of EIT images included: anatomico-topographical correlation of images; visual estimation of images in different scanning planes; searching for focal symptomatic and determination of local conductivity; digital processing of images – determination of relative conductivity of healthy and ill lung, statistical analysis of conductivity values (average value, standard deviation, estimation of difference certainty according to Student criterion).

Results

3.1 Images

EIT image presents tissues conductivity in grey scale. Changing from dark to light corresponds to changing from low conductivity to high. The most illustrative examples are EIT images of persons with opposite changes in lungs: norm, one lung absence, hypo-aeration, hyper-aeration. All images presented in this paper correspond to third intercostal space.

Typical thorax EIT image in norm is presented at Figure 1. It should be noted that the EIT appearance of backbone looks large than lung because the lung on the image is not just compact dark spot (which is rather bronchial tree only), it includes also more light (more conductive) surrounding areas. On the other hand, the low-conductive fat tissues surround the backbone and increase its EIT appearance. The focal symptomatic is absence on this image; alike dark grey scale of both lungs, which means their “airing”. These characteristics are stable at all horizontal scanning planes.

EIT image of thorax after one-sided pneumoektomia (Figure 2) is characterised by mediastinum shift to affection side and absence of the ablated lung at EIT image.

An EIT image of thorax with lung cancer is shown on Figure 3. The changing of affected lung – increasing of area with light tones, which means increasing of conductivity (falling of airing), is observable on the image. Decreasing of aeration in sore lung can cause such changes.

EIT image of thorax organs at one-sided increasing of lungs’ aeration (emphysema) – Figure 4 is characterised by increasing of affected lung’s image, much more dark tones in comparison with healthy lung and shift of mediastinum.

Resolution of EIT is not high enough to localise a cancer focus directly. However, it is possible to determine the typical ventilation disturbance at affected side. During analysis of EIT images the increasing of conductivity and fall of aeration at affected lung side was visualised in 19 experiments from total 22 measurements carried out on patients with lung cancer. Two cases of unconformity were qualified as result of incorrect measurements. Thus, the percentage of matching was 95%. When collating the level of bronchus affection at different scanning planes (levels of 3, 4, 5 intercostal spaces), we have found the fall of aeration at scanning plane corresponding to affected bronchus. In 13 cases it was fall of aeration at 3-rd intercostal space scanning and top-lobe tumour, in 6 cases – at 5-th intercostal space scanning and bottom-lobe tumour.

3.2 Quantitative estimations

All quantitative estimations were carried out using conductivity data reconstructed in "scale" mode, see details section 2.2. With such calibration procedure “conductivity” can be negative sometimes actually (as in case of emphysema, Figure 4). However, quantitative comparison of

these values could give useful information characterising state of lung's tissue. In Table 1 we present the average values and standard deviations of lungs' "conductivity" in each group.

Table 1.

	1 group	2 group	Pneumoektomia	Emphysema
"Conductivity"	0.591±0.229	0.248±0.071	1.101	-0.237

Average conductivity of affected lung (group 1) is greatly higher than conductivity of healthy one (group 2) and this difference is statistically significant.

Discussion

In spite of low spatial resolution static EIT demonstrates sensitivity to lung cancer. The explanation of this phenomenon can be found in changing of conductivity of large areas of tissue around tumour focus. Lung cancer is associated typically with bronchus tree affection, in particular, with narrowing of air opening of bronchial tube. If for example the pipe (bronchus) radius decreasing twice, the resistance to flow increases in 16 times. This causes the regional differences in lungs' aeration. Tumour growth causes fall of aeration in lung region related topographically with affected bronchus. At EIT images the areas with low aeration are characterised by higher conductivity, appearing as light tones of grey scale in lungs' image. According to scanning level (3, 4, 5 intercostal space), where the increased conductivity was detected, it is possible to determine the topographical placement of bronchus tree affection. Quantitative estimations of the images give the statistically significant difference in conductivity of healthy and affected lungs.

We have presented only preliminary data of clinical investigations. Further more detailed investigation in this area could contribute to the entering of the chest EIT to the practical medicine. In particular, first results demonstrate potential for the safe and accessible initial lung diagnosis on the trivial level: "healthy" - "ill" by the visual comparison of left and right lungs on static EIT images.

References

Barber D C and Brown B H 1984 Applied potential tomography *J. Phys. E: Sci. Instrum.* **17** 723-33

Harris N D, Suggett A J, Barber D C and Brown B H 1987 Applications of applied potential tomography (APT) in respiratory medicine *Clin. Phys. Physiol. Meas.* **8** (Supplement A) 155-65

Cherepenin V A, Korjenevsky A V, Kornienko V N, Kultiasov M Y, Kultiasov Y S 1995 The electrical impedance tomograph: new capabilities *Proc. 9th Int. Conf. On Electrical Bio-Impedance (Heidelberg, 1995)* 430-33

Eyuboglu B M, Oner A F, Baysal U, Biber C, Keyf A I, Yilmaz U and Erdogan Y 1995 Application of electrical impedance tomography in diagnosis of emphysema – a clinical study *Physiol. Meas.* **16** (Supplement 3A) A191-A211

Frerichs I, Hahn G, Schiffmann H, Berger C and Hellige G Monitoring regional lung ventilation by functional electrical impedance tomography during assisted ventilation *Ann. NY Acad. Sci.* **873** 493-505

Korjenevsky A V 1995 Reconstruction of absolute conductivity distribution in electrical impedance tomography *Proc. 9th Int. Conf. On Electrical Bio-Impedance (Heidelberg, 1995)* 532-35

Korjenevsky A V, Kornienko V N, Kultiasov M Y, Kultiasov Y S and Cherepenin V A 1997 *Pribory i Tekhnika Experimenta* No 3 133-40 (Engl. transl. Korzhenevskii A V, Kornienko V N, Kul'tiasov M Y, Kul'tiasov Y S and Cherepenin V A Electrical impedance computerized tomograph for medical applications *Instruments and Experimental Techniques* **40** 415-21)

Korjenevsky A V, Cherepenin V A, Kornienko V N and Kultiasov Y S 1998 Electrical impedance tomography with non-adjacent current injection and back projection image reconstruction *Proc. 10th Int. Conf. On Electrical Bio-Impedance (Barcelona, 1998)* 451-53

Leathard A D, Brown B H, Campbell J, Zhang F, Morice A H and Tayler D 1994 A comparison of ventilatory and cardiac-related changes in EIT images of normal human lungs and of lungs with pulmonary emboli *Physiol. Meas.* **15** (Supplement A) A137-A146

FIGURE CAPTIONS

Figure 1. Static EIT image of human thorax at norm: 1 – lungs, 2 - heart and mediastinum, 3 – spinal column, 4 - chest bone.

Figure 2. Thorax EIT image of patient after one-sided pneumoektomia.

Figure 3. EIT image of thorax at one-sided fall of lungs' aeration related with lung cancer.

Figure 4. EIT image of thorax at one-sided increasing of lungs' aeration (emphysema).

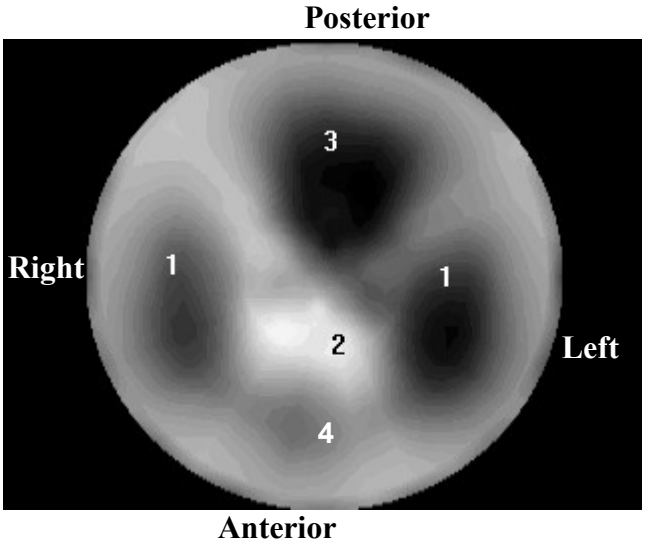

Figure 1.

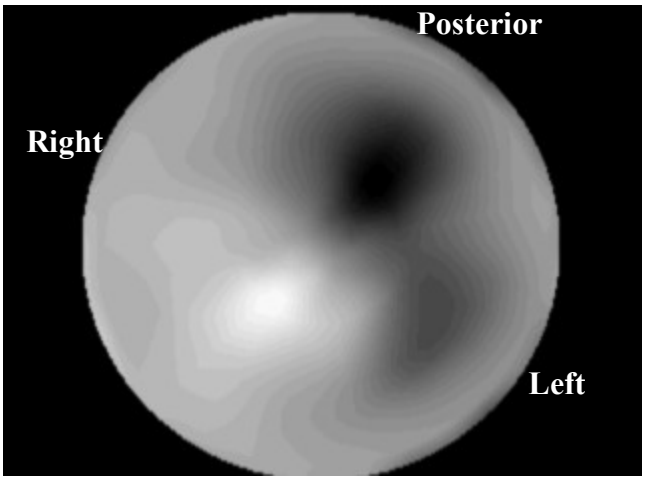

Figure 2.

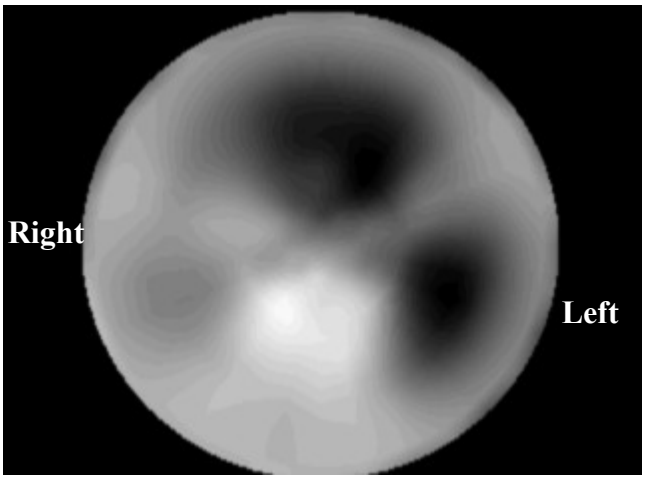

Figure 3.

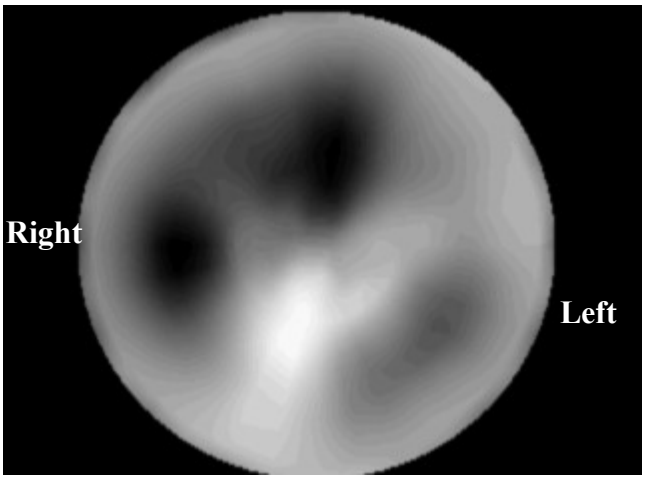

Figure 4.

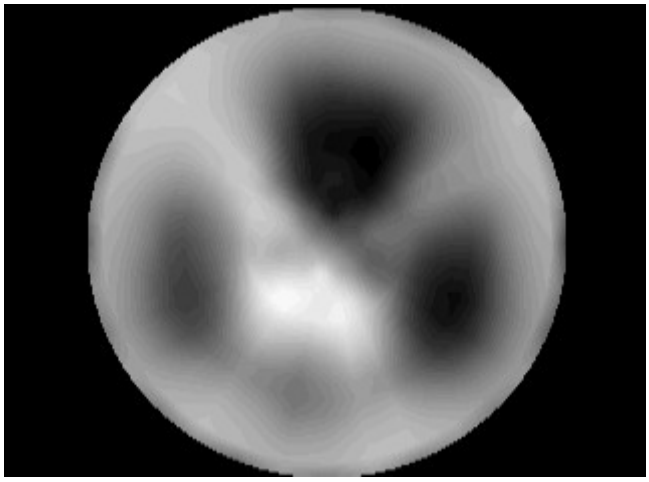

Figure 1. (without marks)